Eur. Phys. J. A **12**, 91–101 (2001)

THE EUROPEAN PHYSICAL JOURNAL A

Hadronic decays of N and Δ resonances in a chiral quark model

L. Theußl[1,a], R.F. Wagenbrunn[2], B. Desplanques[1], and W. Plessas[3]

[1] Institut des Sciences Nucléaires (Unité Mixte de Recherche CNRS-IN2P3, UJF) F-38026 Grenoble Cedex, France
[2] Dipartimento di Fisica Nucleare e Teorica, Università di Pavia and INFN, Pavia 27100, Italy
[3] Institut für Theoretische Physik, Universität Graz, Universitätsplatz 5, A-8010 Graz, Austria

Received: 11 May 2001 / Revised version: 3 July 2001
Communicated by P. Schuck

Abstract. π and η decay modes of light baryon resonances are investigated within a chiral quark model whose hyperfine interaction is based on Goldstone-boson exchange. For the decay mechanism a modified version of the $^3P_0$ model is employed. Our primary aim is to provide a further test of the recently proposed Goldstone-boson exchange constituent quark model. We compare the predictions for π and η decay widths with experiment and also with results from a traditional one-gluon exchange constituent quark model. The differences between nonrelativistic and semirelativistic versions of the constituent quark models are outlined. We also discuss the sensitivity of the results on the parameterization of the meson wave function entering the $^3P_0$ model.

PACS. 12.39.Pn Potential models – 13.30.Eg Hadronic decays – 14.20.Gk Baryon resonances with $S = 0$

1 Introduction

The investigation of hadronic transitions of baryon resonances is currently of high interest [1]. On the experimental side, there are considerable efforts to measure these reactions in order to gain more and improved data on the resonance states. On the theoretical side, a quantitative description of the very details of the baryon ground and excited states represents a big challenge for all hadron models. Obviously the aim is to reach a comprehensive understanding of the low-energy hadron phenomenology on the basis of quantum chromodynamics (QCD).

A promising approach to low-energy hadrons consists in constituent quark models (CQMs). Starting from rudimentary attempts more than two decades ago, one has constantly improved the description and gained a lot of insight into the properties of hadrons at low and intermediate energies. Evidently, CQMs can at most be effective models of QCD in a domain where the fundamental theory is not (yet) accurately solvable. However, the concept of constituent quarks, in the beginning mainly motivated by symmetry considerations of hadron multiplets, nowadays gets more and more justified on the basis of QCD itself, as indicated by quenched lattice simulations [2,3]. It appears that the spontaneous breaking of chiral symmetry (SBχS) of QCD is responsible for the generation of constituent quarks as quasiparticles below a certain scale. Numerous evidences hint to a chirally broken phase (Nambu-Goldstone mode) of QCD.

[a] e-mail: lukas@isn.in2p3.fr

Recently a chiral constituent quark model (CCQM) has been proposed that exploits the SBχS of QCD in deducing the hyperfine interaction of constituent quarks in light and strange baryons [4]. It relies on constituent quark and Goldstone-boson fields as the relevant degrees of freedom in an effective interaction Lagrangian [5]. The so-called Goldstone-boson exchange (GBE) CQM introduces new symmetry properties into the hyperfine interaction of constituent quarks, which are rather different from traditional CQMs advocating one-gluon exchange (OGE) dynamics [6]. The GBE CQM has turned out rather successful in producing an accurate description of the whole light and strange baryon phenomenology in a unified framework [4].

However, the reproduction of the baryon ground-state and resonance energies is just one item that has to be fulfilled by a successful hadron model. In addition, any CQM should also provide for a description of dynamical properties accessible through all types of reaction processes. Here we specifically study the performance of the GBE CQM in hadronic decays of N and Δ resonances. Thereby we produce a further test of the reliability of the new kind of hyperfine interaction based on GBE.

We obtain three-quark wave functions for all the needed ground and excited baryon states by solving a differential Schrödinger-type equation with the stochastic variational method (SVM) [7]. These wave functions are then employed within a certain decay model in order to calculate partial widths for π and η decays of N and Δ resonance states up to $\sim$1.8 GeV. For the decay mech-

anism, we use a modified version of the $^3P_0$ model, which provides a microscopic description of the decay process, allowing one to take into account the internal structure of the emitted meson. Thereby it improves upon the elementary emission model (EEM) which can be recovered in the approximation of a point-like meson. We compare the results to the experimental data and contrast them to an analogous study along a traditional version of the OGE CQM [8]. Our main aim is twofold: First we want to see how well the available data are reproduced by the GBE CQM, and second we wish to find possible differences between the two distinct types of CQMs.

In the following section we give a short description of the quark models used in the present study. We specify their parameterizations both in a nonrelativistic and a semirelativistic framework. In sect. 3 we explain the specific decay model we use here and give the pertinent formulae for the calculation of partial decay widths. The results are presented in sect. 4 along with a discussion of their sensitivity on different ingredients both in the CQMs and in the decay model. Our conclusions are given in sect. 5.

2 Constituent quark models

Let us start by specifying the constituent quark models we use in the present study. The total three-quark Hamiltonian for baryons has the general form

$$H = H_0 + V, \tag{1}$$

where H_0 is the kinetic-energy operator and V contains all the quark-quark interactions, *i.e.* confinement plus hyperfine potentials. For constituent quarks with effective masses of the order of a few hundred MeV the kinetic-energy operator should be taken in relativistic form

$$H_0^{\rm SR} = \sum_{i=1}^{3} \sqrt{\vec{p}_i^{\,2} + m_i^2}, \tag{2}$$

with m_i the masses and $\vec{p}_i$ the 3-momenta of the constituent quarks. A free Hamiltonian as in eq. (2) leads to the so-called relativized or semirelativistic (SR) CQM [9]. It helps to avoid pathologies that usually appear in nonrelativistic constituent quark models [6]. We devote our attention primarily to the SR versions of the GBE and OGE CQMs as described below. Nevertheless, in order to provide a connection to previous studies of hadronic baryon decays, we consider also nonrelativistic (NR) versions of the two types of CQMs, which use the kinetic-energy operator in the form

$$H_0^{\rm NR} = \sum_{i=1}^{3} \left(m_i + \frac{\vec{p}_i^{\,2}}{2m_i} \right). \tag{3}$$

2.1 GBE constituent quark model

For the CCQM relying on GBE dynamics we specifically adhere to the version published in ref. [4]. It comes with a mutual quark-quark interaction

$$V_{ij} = V_{\rm conf} + V_\chi, \tag{4}$$

with a confinement potential in linear form

$$V_{\rm conf}(r_{ij}) = V_0 + C r_{ij} \tag{5}$$

and the chiral interaction consisting of only the spin-spin part of the pseudoscalar-meson exchange

$$V_\chi(\vec{r}_{ij}) = \left[\sum_{F=1}^{3} V_\pi(\vec{r}_{ij}) \lambda_i^F \lambda_j^F + \sum_{F=4}^{7} V_K(\vec{r}_{ij}) \lambda_i^F \lambda_j^F + V_\eta(\vec{r}_{ij}) \lambda_i^8 \lambda_j^8 + \frac{2}{3} V_{\eta'}(\vec{r}_{ij}) \right] \vec{\sigma}_i \cdot \vec{\sigma}_j. \tag{6}$$

Here $\vec{\sigma}_i$ are the Pauli spin matrices and λ_i the Gell-Mann flavor matrices of the individual quarks. The meson-exchange potentials are parameterized in the form

$$V_\gamma(\vec{r}_{ij}) = \frac{g_\gamma^2}{4\pi} \frac{1}{12 m_i m_j} \left\{ \mu_\gamma^2 \frac{e^{-\mu_\gamma r_{ij}}}{r_{ij}} - \Lambda_\gamma^2 \frac{e^{-\Lambda_\gamma r_{ij}}}{r_{ij}} \right\}, \quad (\gamma = \pi, K, \eta, \eta'), \tag{7}$$

with μ_γ the meson masses, g_γ the meson-quark coupling constants, and Λ_γ the cut-off parameters resulting from the smearing of the δ-functions (for details see refs. [4] and also [6]). A single coupling constant g_8 is taken for all pseudoscalar octet mesons. In case of the SR GBE CQM it is set equal to the pion-quark coupling constant, whose value can be deduced from πN phenomenology via the Goldberger-Treiman relation. The coupling constant g_0 for the singlet η' is determined differently by a fit to the baryon spectra. The cut-offs Λ_γ are assumed to scale with the phenomenological meson masses according to the simple rule

$$\Lambda_\gamma = \Lambda_0 + \kappa \mu_\gamma. \tag{8}$$

The strength and depth of the confinement potential (5) are determined by C and V_0, respectively. While these values have also been fitted to the baryon spectra, it is interesting to remark that for the SR GBE CQM the strength C comes out just in consistency with the QCD string tension. The parameter V_0 is needed merely to fix the ground-state level at the nucleon mass. All the parameter values are collected in table 1.

Table 1 also contains the parameters for a NR version of the GBE CQM [10], *i.e.* when the potential (4) is used together with the kinetic-energy operator (3). While the description of the N and Δ is achieved with a similar quality (cf. fig. 1 and table 3, below), it is worthwhile to note the drastically different values of the fitted parameters (first 6 lines in table 1) in both the confinement and chiral interactions. In particular, the confinement potential becomes unrealistically weak, while the hyperfine potential gets much enhanced as compared to the SR case.

Table 1. Parameters of the GBE CQM for the semirelativistic [4] and nonrelativistic [10] parameterizations. The first six have been fitted to the baryon spectra (including hyperons) while the last four were given currently accepted or experimental values.

Parameters	SR	NR
$\frac{g_8^2}{4\pi}$	0.67	1.24
$(g_0/g_8)^2$	1.34	2.23
Λ_0 (fm^{-1})	2.87	5.82
κ	0.81	1.34
C (fm^{-2})	2.33	0.77
V_0 (MeV)	−416	−112
$m_u = m_d$ (MeV)	340	340
μ_π (MeV)	139	139
μ_η (MeV)	547	547
$\mu_{\eta'}$ (MeV)	958	958

2.2 OGE constituent quark model

For the purpose of comparison to a different kind of quark-quark dynamics we employ a traditional OGE CQM. Specifically, it is the model following Bhaduri, Cohler, and Nogami (BCN) [8]. In this case the total potential has the form

$$V_{ij} = V_0 + C r_{ij} - \frac{2b}{3r_{ij}} + \frac{\alpha_s}{9 m_i m_j} \Lambda^2 \frac{e^{-\Lambda r_{ij}}}{r_{ij}} \vec{\sigma}_i \cdot \vec{\sigma}_j, \qquad (9)$$

i.e. it consists of a short-range Coulomb term, a linear confinement, and a flavor-independent spin-spin interaction. The parameter values for the original BCN potential were determined from a fit to the meson spectra, and they were also used in a previous study [11]. We have redetermined the model parameters from a fit to the baryon spectra. Their values are summarized in table 2, from where it can be seen that they differ from the parameter set used in ref. [8], specifically in the NR case.

Again the spectra are produced in quite a similar manner by both the SR and NR versions (cf. fig. 2 and table 3). Of course, the typical difficulties of OGE CQMs appear, *e.g.*, with respect to the relative orderings of the lowest positive- and negative-parity excitations.

Before concluding this section a few remarks about the above versions of the GBE and OGE CQMs are in order.

Table 2. Parameters of the OGE CQM after BCN [8] for the semirelativistic and nonrelativistic parameterizations. Four parameters were determined from a fit to the nonstrange baryon spectra (b and α_s are assumed to be equal) while the quark masses are the same as in the original BCN model.

Parameters	SR	NR
$b = \alpha_s$	0.57	0.825
Λ (fm^{-1})	2.7	5
C (fm^{-2})	3.12	2.26
V_0 (MeV)	−409	−366
$m_u = m_d$ (MeV)	337	337

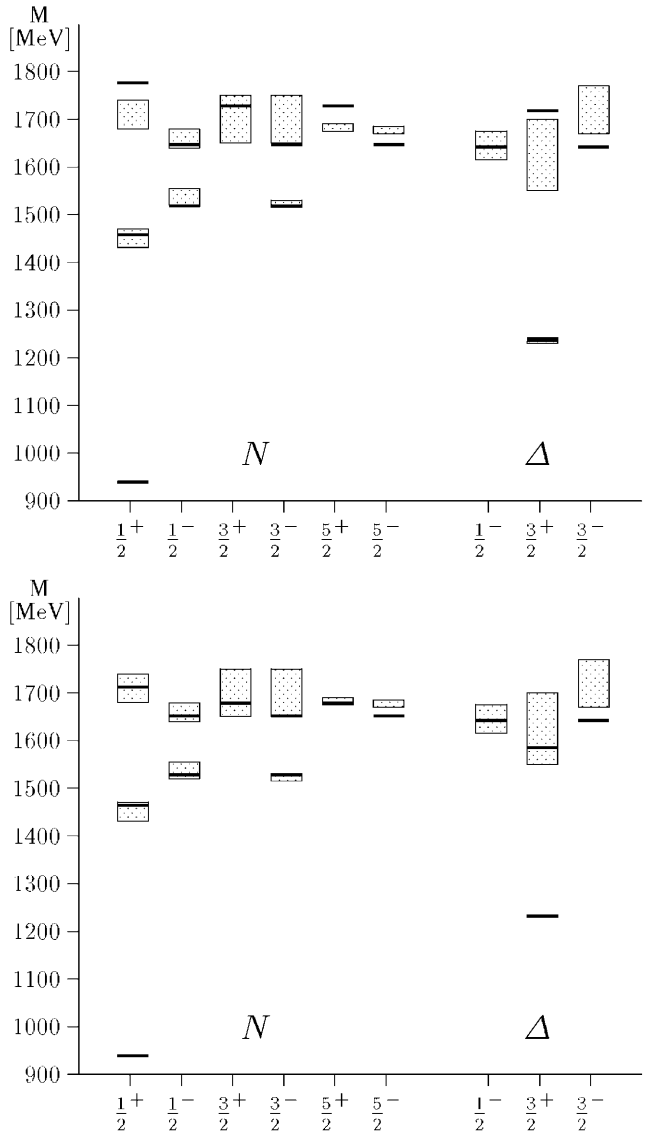

Fig. 1. Energy levels (solid lines) of the lowest N and Δ states with total angular momentum and parity J^P for the semirelativistic (top) and the nonrelativistic versions (bottom) of the GBE CQM. The shadowed boxes represent the experimental values with their uncertainties according to the most recent compilation of the Particle Data Group [12].

For both cases the models considered here contain only the most important ingredients for the quark-quark interactions in baryon spectra, *i.e.* essentially confinement plus spin-spin hyperfine interactions. However, both the GBE and OGE models bring about also further force components, such as central, tensor, and spin-orbit forces. While their influence must be minor in the N and Δ spectra (as demanded by their phenomenological structure) they could be of enhanced importance in dynamical observables such as hadronic widths, nucleon form factors, etc. In the study we present below, we shall thus essentially explore the effects of the most prominent parts of the inter-quark forces. The GBE CQM has so far been published only with the spin-spin part of the quark-quark interaction [4], [10].

Table 3. Energies of baryon resonances predicted by the different CQMs considered in this work. For all models the nucleon mass is 939 MeV.

N^*	J^π	M (MeV)			
		GBE SR	GBE NR	OGE SR	OGE NR
N_{1440}	$\frac{1}{2}^+$	1459	1465	1578	1743
N_{1710}	$\frac{1}{2}^+$	1776	1712	1860	1925
Δ_{1232}	$\frac{3}{2}^+$	1240	1232	1232	1232
Δ_{1600}	$\frac{3}{2}^+$	1718	1585	1855	1967
N_{1520}-N_{1535}	$\frac{3}{2}^-$-$\frac{1}{2}^-$	1519	1529	1521	1531
N_{1650}-N_{1675}-N_{1700}	$\frac{1}{2}^-$-$\frac{5}{2}^-$-$\frac{3}{2}^-$	1647	1652	1691	1681
Δ_{1620}-Δ_{1700}	$\frac{1}{2}^-$-$\frac{3}{2}^-$	1642	1642	1621	1654
N_{1680}-N_{1720}	$\frac{5}{2}^+$-$\frac{3}{2}^+$	1728	1679	1858	1883

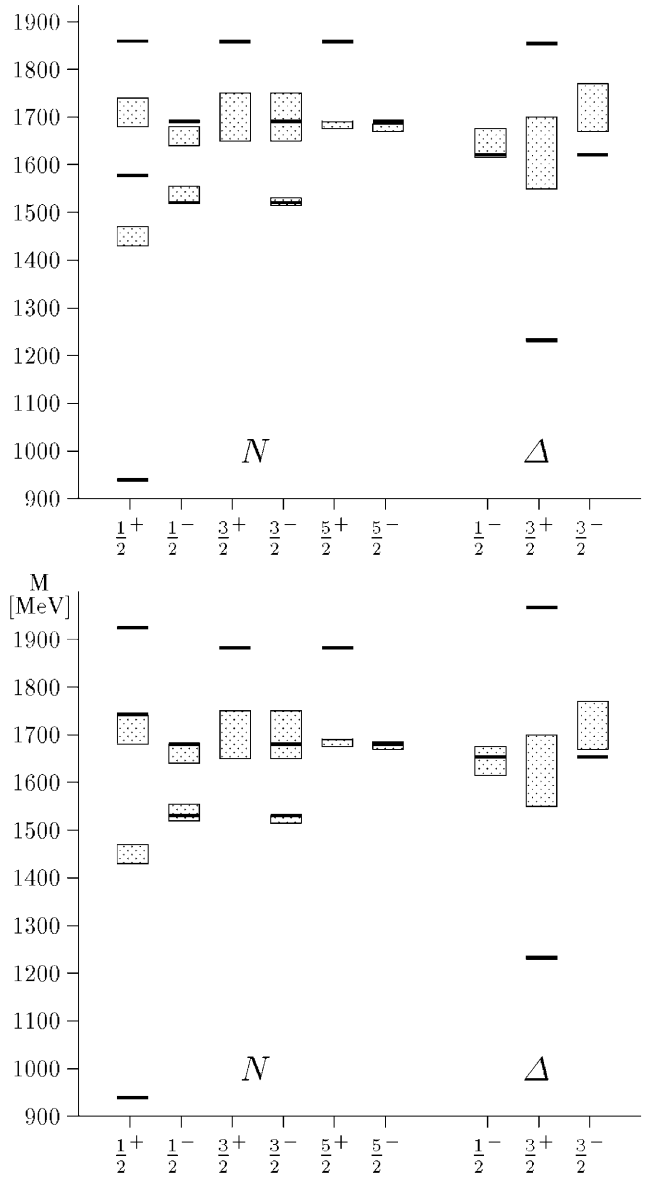

Fig. 2. As fig. 1 but for the OGE CQM after BCN in the semirelativistic (top) and nonrelativistic versions (bottom).

For consistency in the comparison, also the OGE CQM is considered only with the spin-spin component.

3 The $^3P_0$ model for strong decays

Investigations of hadronic decays have a long history with first attempts dating back to the early times of quark models. Still, the definite form of the decay operator is not yet known. Specific difficulties arising in strong interaction decays are connected with the extended sizes of both the baryons and the mesons involved in the decay process. Obviously one would require a reliable microscopic model that consistently accounts for the description of both the hadron states and the decay mechanism.

The simplest ansatz for the decay operator is furnished by the elementary emission model (EEM) [13–15]. Therein a point-like meson is produced by a single constituent quark in the decaying baryon state. Evidently, this assumption leads to shortcomings, as found in a number of investigations with various CQMs (cf., for example, ref. [16]). While the model usually does well for the so-called "structure-independent" transitions (in the terminology of ref. [17]), it completely fails for transitions from radial excitations to the ground state. Such findings obtained before in case of the OGE CQM have subsequently also been confirmed by a preliminary study of baryon decays within the semirelativistic GBE CQM in ref. [18].

An improved description of hadron decays is provided by the $^3P_0$ (or quark-pair creation) model. Here a $q\bar{q}$ pair is created from the vacuum and by a subsequent rearrangement the final meson and baryon states are produced. The $^3P_0$ model naturally allows to implement the extended structure of the emitted meson. Thereby, this model provides also a reasonable description of transitions involving radial excitations, without pretending to give the final answer for a correct treatment of the decay process of light baryon resonances. By definition, the quark-antiquark pair must carry the quantum numbers of the vacuum, *i.e.* it is a color and flavor singlet, has positive P- and C-parity, total angular momentum $J = 0$ and carries total linear momentum zero. From $P = -(-1)^L$ and $C = (-1)^{L+S}$

one deduces as the simplest choice $L = S = 1$. The corresponding transition operator for the decay can thus be expressed as [19]

$$\begin{aligned}\mathcal{T} &= \gamma \sum_{i,j} \int \mathrm{d}^3p_q \mathrm{d}^3p_{\bar{q}} \delta(\vec{p}_q + \vec{p}_{\bar{q}}) \\ &\times \sum_m \left[C^{00}_{1m1-m} \mathcal{Y}^m_1(\vec{p}_{\bar{q}} - \vec{p}_q) (\chi^{-m}_1(i,j) \phi_0(i,j)) \right] \\ &\times b^\dagger_i(\vec{p}_q) d^\dagger_j(\vec{p}_{\bar{q}}) \,, \end{aligned} \tag{10}$$

where, in evident notation, the momenta refer to the quark and antiquark states created by the operators $b^\dagger_i$ and $d^\dagger_j$, respectively. $\mathcal{Y}^M_L(\vec{p}) = p^L Y^M_L(\hat{p})$ is a solid harmonics function, which gets coupled with the triplet spin wave function χ to give $J = 0$. ϕ_0 is the flavor singlet wave function and the summation $\sum_{i,j}$ runs over spin and flavor indices. The pair creation constant γ is a dimensionless coefficient which is the only adjustable parameter of the model (apart from factors entering an eventual parameterization of the meson wave functions). Note that in eq. (10) we have omitted a factor 3 in front of this constant which is frequently used to cancel a factor 1/3 coming from the matrix element of color wave functions, which are not written out explicitly here.

The transition matrix element for the process $B \to B'M$ is then expressed as

$$\begin{aligned}&\langle B'M \mid \mathcal{T} \mid B \rangle \equiv \langle B'M \mid H \mid B \rangle = \\ &3\gamma \sum_m C^{00}_{1m1-m} \mathcal{I}_m =: \delta(\vec{P} - \vec{P}' - \vec{q}) \mathcal{A} \,. \end{aligned} \tag{11}$$

Here, the factor 3 comes from the different possibilities of rearranging the quarks in the initial and final state, taking into account the symmetry of the wave functions. The momentum integral of eq. (11) takes the form

$$\begin{aligned}\mathcal{I}_m = &\int \mathrm{d}^3p_1 \mathrm{d}^3p_2 \mathrm{d}^3p_3 \mathrm{d}^3p_4 \mathrm{d}^3p_5 \mathcal{Y}^m_1(\vec{p}_4 - \vec{p}_5) \delta(\vec{p}_4 + \vec{p}_5) \Phi^{-m}_{\mathrm{pair}} \\ &\times [\Psi_{B'}(\vec{p}_1, \vec{p}_2, \vec{p}_4) \Phi_{B'}]^* \, [\Psi_M(\vec{p}_3, \vec{p}_5) \Phi_M]^* \\ &\times [\Psi_B(\vec{p}_1, \vec{p}_2, \vec{p}_3) \Phi_B] \,. \end{aligned} \tag{12}$$

Here, $\vec{p}_1, \vec{p}_2, \vec{p}_3$ are the individual quark momenta of the initial baryon B which sum up to a total momentum $\vec{P} = \sum_{i=1}^3 \vec{p}_i = 0$ in the rest frame of B. The meson carries away the momentum $\vec{q} = \vec{p}_3 + \vec{p}_5$, and the residual baryon B' has momentum $\vec{P}' = \vec{p}_1 + \vec{p}_2 + \vec{p}_4 = -\vec{q}$, due to momentum conservation in the decay process. Finally, we denoted the combined spin-isospin wave functions involved in the decay process by Φ.

In a next step, one separates the center-of-mass and relative motions in all hadron wave functions, what permits to carry out some of the integrations in eq. (12):

$$\begin{aligned}\mathcal{I}_m = \delta(\vec{P} - \vec{P}' - \vec{q}) &\int \mathrm{d}^3p_x \, \mathrm{d}^3p_y \, \mathcal{Y}^m_1(2\vec{q} + 2\vec{p}_y) \, \Phi^{-m}_{\mathrm{pair}} \\ &\times \left[\Psi_{B'} \left(\vec{p}_x, \frac{2}{3}\vec{q} + \vec{p}_y \right) \Phi_{B'} \right]^* \left[\Psi_M \left(-\frac{1}{2}\vec{q} - \vec{p}_y \right) \Phi_M \right]^* \\ &\times \left[\Psi_B(\vec{p}_x, \vec{p}_y) \, \Phi_B \right] , \end{aligned} \tag{13}$$

where $\vec{p}_x = \frac{1}{2}(\vec{p}_1 - \vec{p}_2)$ and $\vec{p}_y = \frac{1}{3}(2\vec{p}_3 - \vec{p}_1 - \vec{p}_2)$ are the momenta conjugate to the Jacobi coordinates $\vec{x}$ and $\vec{y}$.

In ref. [11], it was observed that the $^3P_0$ model can be modified so as to reproduce the EEM in the limit of a point-like meson. Taking also into account a relativistic boost effect, this requires the replacements

$$\gamma \longrightarrow \gamma \sqrt{\frac{\mu}{\omega}} \,, \tag{14}$$

$$\mathcal{Y}^m_1(2\vec{q} + 2\vec{p}_y) \longrightarrow \mathcal{Y}^m_1 \left(\left[1 + \frac{\omega}{2m} \right] \vec{q} + \frac{\omega}{m} \vec{p}_y \right) , \tag{15}$$

where μ is the mass of the emitted meson and $\omega = \sqrt{\mu^2 + \vec{q}^2}$ its energy.

The partial decay width is then obtained by

$$\Gamma = \frac{1}{\pi} \frac{q \, E \, \omega}{M_B} \mid \mathcal{A} \mid^2 , \tag{16}$$

where M_B is the mass of the decaying resonance, E the energy of the final-state baryon, and $\mathcal{A}$ is defined by eq. (11). In eq. (16) one still has to sum over final and to average over initial spin-isospin channels.

For the meson wave function in configuration space we first adopt a simple parameterization of the Gaussian type

$$\Psi_G(\vec{r}) = \frac{1}{(\pi R^2)^{3/4}} \exp\left(-\frac{r^2}{2R^2} \right) , \tag{17}$$

where the parameter R^2 is related to the mean square radius of the meson by $\langle r^2 \rangle = \frac{3}{2} R^2$. While facilitating the calculations, this choice certainly cannot be regarded as a realistic representation of a meson wave function. We shall therefore investigate the influence of a different analytic form of meson wave functions on the baryon decay widths.

From the Fourier transform of the electromagnetic pion form factor, one can deduce a pion wave function that takes a Yukawa-like form:

$$\Psi_Y(\vec{r}) = \frac{1}{\sqrt{4\pi}} \frac{m}{\sqrt{r}} \exp\left(-\frac{mr}{2} \right) . \tag{18}$$

Here the parameter m is related to the mean square radius of the meson by $\langle r^2 \rangle = 6/m^2$. Even if it is not physically meaningful, this expression may serve as a comparison to the Gaussian form.

A graphical representation of the meson wave functions is given in fig. 3, where we compare the above forms to the wave function that follows from the original potential of Bhaduri *et al.* [8]. It can be seen that the exact wave function lies just between the extreme choices of a Yukawa and a Gaussian form. The parameters of eqs. (17) and (18) have been fitted to give the same root mean square radius for the pion as the wave function from the potential of ref. [8], that is $r_\pi = 0.565$ fm. For simplicity we use the same parameterization for the wave function of the η-meson.

Applying the $^3P_0$ model to wave functions stemming from the GBE dynamics, one is quite immediately faced with the apparent paradox that one describes the pion at the same time as an elementary field at the level of the

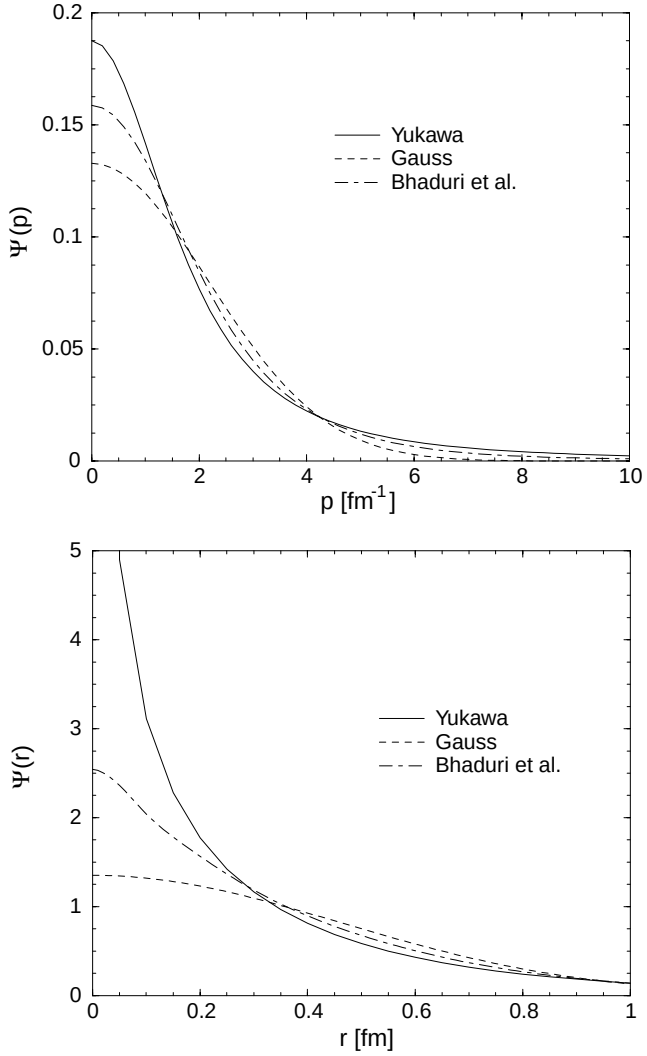

Fig. 3. Meson wave functions in momentum (top) and configuration space (bottom). Gaussian and Yukawa forms are compared to the exact wave function following from the original quark-antiquark potential of Bhaduri *et al.* [8].

interaction and as a $q\bar{q}$ bound state at the level of decays. But then it has to be stated that even in the GBE, the pion is not really a fundamental field but still a bound state of quark and anti-quark, whose Goldstone (quasiparticle) character arises from the spontaneous breaking of chiral symmetry. Only in practical parameterizations one starts from a phenomenological Lagrangian including an effective pion field in order to get the proper symmetry structure of the interaction. It would be interesting to establish a relationship between the spatial extension of the pion, as implied by the form factor in the interaction, see eq. (8), and the pion wave function, like eq. (17); as well as between the corresponding meson-baryon vertices and coupling strength. However, the form factor in the interaction rather represents a quark extension. The above-mentioned relationship is therefore not trivial, since it would require a more microscopic description of both the interaction and the decay process. On the effective level we work at, the parameters assumed in different models have to be considered purely phenomenological.

4 Results for π and η partial decay widths

In this section we shall present the results for the π and η decay modes of N and Δ resonances, as predicted by the CQMs specified in sect. 2. At the beginning we discuss some features of the baryon wave functions.

4.1 Three-quark wave functions

The solutions of the three-quark Hamiltonians have been obtained by solving the corresponding Schrödinger-type differential equations with the SVM [7]. The accuracy that is attained with respect to the eigenenergies in table 3 is generally within a few percent even for the highest states considered. In this context the SVM was carefully conterchecked with complementary approaches, such as the Faddeev method [6,20]. Another measure for the accuracy of the solution of the three-quark problem is the mean square radius of the wave function. In the context of the present work this quantity is also useful for understanding some general characteristics of the results for decay widths, which are connected to the baryon sizes. In table 4 we therefore quote mean square radii of the N and Δ ground-state wave functions for the CQMs considered. The values refer to the case with point-like constituent quarks. Therefore they are probably not realistic and must not be compared to experimental values. They are only useful to get insight into the relative extensions of the wave functions from each CQM.

Obviously, the values of the mean square radii are all rather small. Within each type of CQM, GBE or OGE, they are smaller in the semirelativistic cases, as it was already observed in ref. [9]. This may be viewed as a consequence of the stronger confinement generally needed in the semirelativistic CQMs. Inspection of the absolute magnitudes of the relevant quantities in tables 1, 2, and 4 shows, however, that confinement cannot be the only factor determining the mean square radii of the wave functions (note that the differences in confining strengths are much larger for the GBE parameterizations). A smaller extension of the baryon wave functions evidently implies even larger values for internal momenta (in the semirelativistic CQMs). This will help to explain certain results for decay widths involving high momenta in the next sections.

Table 4. Mean square radii of N and Δ from the various CQMs, assuming point-like constituent quarks.

	GBE SR	GBE NR	OGE SR	OGE NR
$\langle r_N^2 \rangle$ (fm^2)	0.092	0.134	0.076	0.219
$\langle r_\Delta^2 \rangle$ (fm^2)	0.152	0.172	0.115	0.288

Table 5. Decay widths of baryon resonances for the GBE and OGE constituent quark models both in nonrelativistic and semirelativistic parameterizations. A Gaussian-type meson wave function with $r_\pi = r_\eta = 0.565$ fm was used along with a modified $^3P_0$ decay model. Experimental data are from ref. [12]; for the quoted uncertainties refer to the text.

N^*	J^π	$\Gamma(N^* \to N\pi)$ (MeV)					$\Gamma(N^* \to N\eta)$ (MeV)				
		GBE SR	GBE NR	OGE SR	OGE NR	Exp.	GBE SR	GBE NR	OGE SR	OGE NR	Exp.
N_{1440}	$\frac{1}{2}^+$	517	258	1064	161	$(227 \pm 18)^{+70}_{-59}$			6	10	
N_{1710}	$\frac{1}{2}^+$	54	14	202	8	$(15 \pm 5)^{+30}_{-5}$	26	4	50	10	
Δ_{1232}	$\frac{3}{2}^+$	120	120	120	120	$(119 \pm 1)^{+5}_{-5}$					
Δ_{1600}	$\frac{3}{2}^+$	43	34	174	14	$(61 \pm 26)^{+26}_{-10}$					
N_{1520}	$\frac{3}{2}^-$	131	161	108	168	$(66 \pm 6)^{+9}_{-5}$	0	0	0	0	
N_{1535}	$\frac{1}{2}^-$	336	75	462	109	$(67 \pm 15)^{+55}_{-17}$	64	64	64	64	$(64 \pm 19)^{+76}_{-15}$
N_{1650}	$\frac{1}{2}^-$	53	5	87	8	$(109 \pm 26)^{+36}_{-3}$	113	68	140	94	$(10 \pm 5)^{+4}_{-1}$
N_{1675}	$\frac{5}{2}^-$	34	35	40	52	$(68 \pm 8)^{+14}_{-4}$	2	4	3	5	
N_{1700}	$\frac{3}{2}^-$	6	6	7	9	$(10 \pm 5)^{+3}_{-3}$	0	1	1	1	
Δ_{1620}	$\frac{1}{2}^-$	26	3	41	5	$(38 \pm 8)^{+8}_{-6}$					
Δ_{1700}	$\frac{3}{2}^-$	28	29	20	38	$(45 \pm 15)^{+20}_{-10}$					
N_{1680}	$\frac{5}{2}^+$	85	85	149	313	$(85 \pm 7)^{+6}_{-6}$	0	1	2	6	
N_{1720}	$\frac{3}{2}^+$	377	100	689	238	$(23 \pm 8)^{+9}_{-5}$	15	11	30	25	
γ		15.365	14.635	18.015	11.868		5.929	6.682	6.572	4.937	

4.2 π decays

The results for the partial widths of the π decay modes of the N and Δ resonances are shown in table 5. All values have been calculated with the Gaussian-type parameterization of the meson wave function of eq. (17). For the baryons, the theoretical masses have been used as predicted by the different CQMs in table 3. In each case the strength parameter γ introduced into the decay operator in eq. (10) has been adjusted so as to reproduce the $\Delta_{1232} \to N\pi$ decay width. All the other decay widths can then be considered as genuine predictions of the CQMs along the modified $^3P_0$ model.

Table 5 also allows a comparison of the theoretical results to experimental data as compiled by the Particle Data Group (PDG) [12]. For the latter there arise two kinds of uncertainties: First, the total decay width of each resonance is given by a central value and a lower and upper bound. Second, the partial decay width has its own uncertainty. In table 5 we quote the value for the π decay widths deduced from the central value of the total width and first add the uncertainty from the partial decay width itself (numbers inside the parentheses in the last column). Then we indicate also the range of the total decay width by an upper and lower bound. We understand that the total uncertainty in a partial decay width must be estimated by combining both types of uncertainties (inherent separately in the total and partial widths).

Let us now examine the theoretical results in detail. For the N_{1440} $\frac{1}{2}^+$ resonance the SR GBE prediction is obviously too large, whereas the pertinent NR result lies within the experimental error bars. The SR OGE result overshoots the experiment by far, its NR version is also much smaller than the SR one and lies just at the lower end of the experimental error bar. The results for the next $\frac{1}{2}^+$ excitation of the nucleon, the N_{1710}, show a similar relative pattern as the ones for the Roper resonance, though all the values are smaller by about an order of magnitude. The fact that for each case, N_{1440} and N_{1710}, the predictions of the SR parameterizations of both the OGE and GBE models exceed by far their NR counterparts can be readily understood observing the higher-momentum components present in the SR parameterizations, as compared to the NR ones (cf. the discussion of the baryon wave functions in the previous subsection). In case of the OGE SR this effect is enhanced by a phase space that is much too large (due to the bad prediction of the resonance energy).

For the N_{1720} $\frac{3}{2}^+$ resonance the results again have similar characteristics, with the SR cases drastically overshooting the experimental data. Here, however, none of the NR versions can come close to the rather small experimental width. This problem was already encountered in similar analyses [21,22] and may hint to a wrong symmetry assignment (or a strong mixing) of this state. Only for the N_{1680} $\frac{5}{2}^+$ resonance the GBE CQM produces correct results, both in its SR and NR versions. In this case the results from both variants of the OGE CQM are again too high.

For the negative-parity N_{1535} $\frac{1}{2}^-$ resonance the SR results are also much too high, whereas the predictions from the NR versions agree with experiment. For the N_{1650} $\frac{1}{2}^-$ the situation is just reversed. Most remarkably, in all instances the widths of the N_{1535} resonance are larger than

Table 6. Same as table 5 but using a Yukawa-type meson wave function with $r_\pi = r_\eta = 0.565$ fm.

N^*	J^π	$\Gamma(N^* \to N\pi)$ (MeV)					$\Gamma(N^* \to N\eta)$ (MeV)				
		GBE SR	GBE NR	OGE SR	OGE NR	Exp.	GBE SR	GBE NR	OGE SR	OGE NR	Exp.
N_{1440}	$\frac{1}{2}^+$	528	363	1015	204	$(227 \pm 18)^{+70}_{-59}$			6	15	
N_{1710}	$\frac{1}{2}^+$	59	10	179	7	$(15 \pm 5)^{+30}_{-5}$	32	7	51	14	
Δ_{1232}	$\frac{3}{2}^+$	120	120	120	120	$(119 \pm 1)^{+5}_{-5}$					
Δ_{1600}	$\frac{3}{2}^+$	41	49	142	11	$(61 \pm 26)^{+26}_{-10}$					
N_{1520}	$\frac{3}{2}^-$	140	225	109	187	$(66 \pm 6)^{+9}_{-5}$	0	1	0	1	
N_{1535}	$\frac{1}{2}^-$	251	31	412	61	$(67 \pm 15)^{+55}_{-17}$	64	64	64	64	$(64 \pm 19)^{+76}_{-15}$
N_{1650}	$\frac{1}{2}^-$	39	1	78	3	$(109 \pm 26)^{+36}_{-3}$	110	59	138	86	$(10 \pm 5)^{+4}_{-1}$
N_{1675}	$\frac{5}{2}^-$	35	42	40	55	$(68 \pm 8)^{+14}_{-4}$	3	6	3	7	
N_{1700}	$\frac{3}{2}^-$	6	7	7	9	$(10 \pm 5)^{+3}_{-3}$	1	1	1	1	
Δ_{1620}	$\frac{1}{2}^-$	20	1	39	2	$(38 \pm 8)^{+8}_{-6}$					
Δ_{1700}	$\frac{3}{2}^-$	28	35	21	40	$(45 \pm 15)^{+20}_{-10}$					
N_{1680}	$\frac{5}{2}^+$	98	144	158	379	$(85 \pm 7)^{+6}_{-6}$	1	2	2	10	
N_{1720}	$\frac{3}{2}^+$	276	58	545	132	$(23 \pm 8)^{+9}_{-5}$	14	11	25	22	
γ		15.931	14.741	18.854	11.961		6.608	7.022	7.056	5.469	

the ones of N_{1650}, contrary to experiment, where the N_{1535} width appears to be smaller or is at most as large as the N_{1650} width (taking into account the experimental uncertainties). Regarding the $L = 1$, $S = \frac{3}{2}$ multiplet N_{1650}-N_{1675}-N_{1700}, one notes that the SR parameterizations give approximately the correct ratios of these widths, as it is expected from the corresponding spin-isospin matrix elements. These features are not found for the NR parameterizations due to the exceedingly small value of the N_{1650} width.

Concerning the negative-parity N excitations, it is interesting to note that certain resonances are more sensible to the different parameterizations than others. Specifically, the S-wave resonances N_{1535} and N_{1650} (and likewise also Δ_{1620}) appear to be "structure dependent" [17]. This behaviour results in widths sometimes orders of magnitudes apart for different models. On the other hand, the D-wave resonances N_{1520}, N_{1675}, and N_{1700} (and likewise also Δ_{1700}) are found to be "structure independent". Their decay widths are practically independent of the underlying spectroscopic model. These properties can be easily understood in the framework of the EEM (see ref. [19] for a thorough discussion), and evidently extend to the $^3P_0$ model, which is qualitatively very similar for orbital excitations.

The decay widths for the Δ resonances are practically all correct for the SR GBE CQM. In case of the other models the one or the other shortcoming appears.

4.3 η decays

Table 5 also gives the results for η decays. Here we use the same spatial part for the meson wave function as for π decays but the constant γ is adjusted so as to reproduce the η decay width of the N_{1535} resonance. Note that this gives values for γ about a factor 3 smaller than for the π decays, in contrast to other works [21], where the same value was employed to describe both the π and η decays. This has several reasons, the most imminent one being the replacement according to eq. (14). Furthermore, we use an unmixed flavor wave function for the η meson, *i.e.* a pure flavor octet state. For nonstrange decays as regarded in this work, a possible mixing would only influence the normalization of this wave function, which can effectively be absorbed into the coupling constant γ. Finally, an important contribution comes from our choice of phase space, as given by eq. (16). We use a fully relativistic prescription and experimental values for the meson masses, in contrast to ref. [21], where a much higher, "effective" value for the pion mass was employed. A quick estimate of the magnitudes of these three effects shows indeed that we end up with about a factor of 3 difference in the constant γ between π and η decays.

The η widths of the Roper resonance N_{1440} for the GBE parameterizations (NR as well as SR) are rigorously zero, since in both cases the theoretically predicted masses lie below the η threshold, in accordance with experiment. For the OGE parameterizations, the decay $N_{1440} \to N\eta$ is possible, the corresponding widths remain rather small, however.

In total, there are four resonances predicted with considerable branching ratios in the η decay channel. Only for the N_{1535} and N_{1650} resonances one can compare to experiment, since these are the only ones with an experimental width assigned by the PDG [12]. The relative magnitudes of the experimental decay widths in both of these cases

Table 7. Same as table 5 but using a Gaussian-type meson wave function with $r_\pi = r_\eta = 0.36$ fm.

N^*	J^π	$\Gamma(N^* \to N\pi)$ (MeV)					$\Gamma(N^* \to N\eta)$ (MeV)				
		GBE SR	GBE NR	OGE SR	OGE NR	Exp.	GBE SR	GBE NR	OGE SR	OGE NR	Exp.
N_{1440}	$\frac{1}{2}^+$	240	69	546	44	$(227 \pm 18)^{+70}_{-59}$			2	4	
N_{1710}	$\frac{1}{2}^+$	6	13	63	26	$(15 \pm 5)^{+30}_{-5}$	9	1	18	4	
Δ_{1232}	$\frac{3}{2}^+$	120	120	120	120	$(119 \pm 1)^{+5}_{-5}$					
Δ_{1600}	$\frac{3}{2}^+$	0	2	24	63	$(61 \pm 26)^{+26}_{-10}$					
N_{1520}	$\frac{3}{2}^-$	89	88	81	137	$(66 \pm 6)^{+9}_{-5}$	0	0	3	0	
N_{1535}	$\frac{1}{2}^-$	584	106	953	195	$(67 \pm 15)^{+55}_{-17}$	64	64	64	64	$(64 \pm 19)^{+76}_{-15}$
N_{1650}	$\frac{1}{2}^-$	122	14	227	28	$(109 \pm 26)^{+36}_{-3}$	128	80	156	109	$(10 \pm 5)^{+4}_{-1}$
N_{1675}	$\frac{5}{2}^-$	26	22	32	46	$(68 \pm 8)^{+14}_{-4}$	1	2	1	3	
N_{1700}	$\frac{3}{2}^-$	4	4	5	8	$(10 \pm 5)^{+3}_{-3}$	0	0	0	1	
Δ_{1620}	$\frac{1}{2}^-$	61	8	106	16	$(38 \pm 8)^{+8}_{-6}$					
Δ_{1700}	$\frac{3}{2}^-$	21	18	17	34	$(45 \pm 15)^{+20}_{-10}$					
N_{1680}	$\frac{5}{2}^+$	50	41	93	226	$(85 \pm 7)^{+6}_{-6}$	0	0	1	3	
N_{1720}	$\frac{3}{2}^+$	489	85	1063	352	$(23 \pm 8)^{+9}_{-5}$	12	8	24	23	
γ		20.575	20.695	22.699	17.997		6.844	10.060	6.430	6.619	

are missed by all theoretical models. This is again reminiscent of the EEM, where a similar effect is found. One may expect that the decays of these resonances are quite sensitive to spin-orbit and/or tensor forces in the quark-quark interaction. The inclusion of these force components would probably improve the description of both $N\pi$ and $N\eta$ decays for these resonances.

In addition to N_{1535} and N_{1650}, also the widths of the N_{1710} and the N_{1720} resonances come out appreciably large. The PDG does not quote any experimental data for these states. This does not necessarily mean that their widths are vanishing or too small to be measured. It may simply be the case that experimental ambiguities do not (yet) allow for a reliable determination. In fact, there are single partial-wave analyses that assign an appreciable η decay width, for example, also to the N_{1710}, see ref. [23].

4.4 Influences of the meson wave function

The modified $^3P_0$ decay model has two decisive ingredients: the pair creation strength γ and the parameter determining the extension of the meson wave function. While the former is merely a multiplicative constant, which may be suitably chosen to scale the overall strength of all decays, the latter is a nonlinear parameter, which may also alter the qualitative features of various predictions. In the following we consider certain different choices of the meson wave functions and examine their influences on the decay widths.

In table 6 we show results for decay widths when employing a Yukawa-like meson wave function, as given by eq. (18), producing the same meson size as the Gaussian parameterization before. We have adjusted the parameter γ again to fit the Δ and N_{1535} widths for $N\pi$ and $N\eta$ decays, respectively. However, as compared to table 5, the values change only little in this case.

By comparing the results in tables 5 and 6 it is immediately seen that the specific form of the meson wave function has only a minor influence on the predictions of the decay widths for the π as well as η decay modes. The qualitative features remain essentially unchanged. We have also performed calculations with the exact meson wave function produced by the potential of Bhaduri *et al.* (as shown in fig. 3). They confirm the conclusion that the type of meson wave function is not decisive, provided its extension (meson radius) is kept the same.

We now focus the attention on the dependence of the results on the size of the meson. The meson wave functions employed in tables 5 and 6 both correspond to a radius of $r_\pi = 0.565$ fm. In the limit $r_\pi \to 0$ one expects to reproduce the results of the EEM. Thus it is interesting to look at an intermediate regime. Table 7 gives the decay widths for the same case as in table 5, but for a Gaussian-type wave function leading to a meson radius as small as 0.36 fm.

First we note that the values for the constant γ obtained in this case are considerably larger than before. This is understandable, since in order to recover the results of the point-like meson limit, one has to compensate for the effect of the δ function, which then replaces the meson wave function. In particular, for the Gaussian form of eq. (17) one has the relation

$$(2\pi)^{\frac{3}{2}}\delta(\vec{r}) = \lim_{R\to 0}\left(\frac{\pi}{R^2}\right)^{\frac{3}{4}}\Psi_G(\vec{r}). \qquad (19)$$

Most of the results for the decay widths are now rather different from before. They follow the general trend to-

wards the predictions typical for the EEM. One of the characteristic results of the EEM is the extremely small decay width of the Roper resonance, as the first radial excitation of the nucleon; it is due to the orthogonality of the initial and final-state wave functions, which is strikingly felt in case of the EEM. The results of table 7 show the corresponding trend rather clearly: for all spectroscopic models the N_{1440} widths come out at least a factor of 2 smaller than before, while one is still rather far away from the point-like limit.

Concerning the η decays one observes that the differences in the widths between the N_{1535} and N_{1650} resonances now increase in all cases. Again this follows the (unpleasant) trend towards the predictions typical for the EEM. As a result it appears favourable to use a decay model that permits the use of meson wave functions with finite extensions.

5 Summary and conclusion

In this work we investigated the theoretical description of π and η decays for N and Δ resonances. In the first instance, we were interested in the predictions of the specific chiral constituent quark model whose hyperfine interaction is based on GBE dynamics [4,10]. A detailed comparison to the modern experimental data base [12] is provided. We also studied the results relative to the predictions by a traditional CQM [8] based on OGE but relying on the same type of force components as the GBE CQM. Furthermore, we investigated the differences between a semirelativistic and a nonrelativistic description of the baryon states for both types of CQMs. For the decay mechanism a modified version of the $^3P_0$ model [11] was employed which improves upon the EEM used in earlier studies [18] and allows one to incorporate a microscopic description of the decay process. We also examined the sensitivity of the results on the ingredients entering the decay operator, notably the analytical form and the extension of the meson wave functions.

From the present results it is still difficult to draw definite conclusions about the quality of the wave functions stemming from different CQMs. In fact, the various decay widths seem to be more determined by the choice of the SR or NR parameterizations rather than by the use of either type of dynamics, GBE or OGE. At this stage, we find a number of gross qualitative features that have been observed already before in similar studies along the classical $^3P_0$ decay model.

It should be recalled that here we have not included spin-orbit or tensor forces into the quark model Hamiltonians, especially because these force components are not yet provided by the published versions of the GBE CQM and we wanted to produce a consistent comparison with the other type of dynamics, namely the one resulting from OGE. Some decay widths are certainly sensitive to tensor and spin-orbit components in the wave functions. In this respect it may have been somewhat premature to make a comparison with experimental data at this stage.

In any case, our study reveals (and confirms previous such findings) that the description of strong decays of baryon resonances within present CQMs is not yet fully satisfactory. While incorporating the effects of the tensor and spin-orbit forces could help in a few cases (where mixing effects are expected to be important), one may not expect that they will solve the problem caused by the large widths obtained in the SR parameterizations. This problem persists in all cases we considered. Similar findings were made in other works [11,21,22]. The reason is probably a large amount of high-momentum components in the wave functions or, equivalently, the smallness of the baryons. In this respect, the better results from the NR CQM also suggest that the weight of the high-momentum components is perhaps too large. The corresponding differences between the NR and SR cases directly originate from the type of kinetic-energy operator employed in the calculation.

On the other hand, one must realize that the $^3P_0$ model may also fall short as it is based on intuitive grounds and lacks a firm theoretic foundation. Further modifications of the corresponding operator, including a form factor [21] or factors $1/E$ [24] have been considered with some success but no spectacular improvement. A consistent microscopic description of the strong-decay processes within the framework of CQMs thus remains a challenging task. The ultimate goal would, of course, be a unified description of the resonance spectra and the hadronic, as well as electromagnetic, transitions with the same dynamical scheme.

The authors are indebted to Fl. Stancu, D. Rebreyend, and J.P. Bocquet for useful discussions. This work was supported by the Scientific-Technical Agreement "Amadée" between Austria and France under contract number II.9 and by the TMR contract ERB FMRX-CT96-0008.

References

1. See, *e.g.*, *N^* Physics and Nonperturbative Quantum Chromodynamics*, in *Proceedings of the Joint ECT*/JLAB Workshop, Trento, 1998*, edited by S. Simula B. Saghai, N.C. Mukhopadhyay, and V.D. Burkert, Few-Body Syst. Suppl. **11** (1999).
2. S. Aoki et al., Phys. Rev. Lett. **82**, 4392 (1999).
3. J.I. Skullerud, A.G. Williams, Phys. Rev. D **63**, 054508 (2001).
4. L.Ya. Glozman, W. Plessas, K. Varga, R.F. Wagenbrunn, Phys. Rev. D **58**, 094030 (1998).
5. L.Ya. Glozman, D.O. Riska, Phys. Rep. **268**, 263 (1996).
6. L.Ya. Glozman, Z. Papp, W. Plessas, K. Varga, R.F. Wagenbrunn, Phys. Rev. C **57**, 3406 (1998).
7. Y. Suzuki, K. Varga, *Stochastic Variational Approach to Quantum-Mechanical Few-Body Problems* (Springer, Berlin, 1998).
8. R.K. Bhaduri, L.E. Cohler, Y. Nogami, Nuovo Cimento A **65**, 376 (1981).
9. J. Carlson, J. Kogut, V.R. Pandharipande, Phys. Rev. D **27**, 233 (1983); **28**, 2807 (1983).
10. L.Ya. Glozman, Z. Papp, W. Plessas, K. Varga, R.F. Wagenbrunn, Nucl. Phys. A **623**, 90c (1997).

11. F. Cano, P. González, S. Noguera, B. Desplanques, Nucl. Phys. A **603**, 257 (1996).
12. Particle Data Group (D.E. Groom et al.), Eur. Phys. J. C **15**, 1 (2000).
13. C. Becchi, G. Morpurgo, Phys. Rev. **149**, 1284 (1966).
14. A. Mitra, M. Ross, Phys. Rev. **158**, 1630 (1967).
15. D. Faiman, A.W. Hendry, Phys. Rev. **173**, 1720 (1968); Phys. Rev. Lett. **44**, 845 (1980).
16. Fl. Stancu, P. Stassart, Phys. Rev. C **39**, 343 (1996).
17. R. Koniuk, N. Isgur, Phys. Rev. D **21**, 1868 (1980).
18. L. Ya. Glozman W. Plessas, L. Theussl, K. Varga, R.F. Wagenbrunn, πN Newslett. **14**, 99 (1998).
19. A. Le Yaouanc, Ll. Oliver, O. Pène, J.-C. Raynal, *Hadron Transitions in the Quark Model* (Gordon and Breach Science Publishers, New York, 1988).
20. Z. Papp, A. Krassnigg, W. Plessas, Phys. Rev. C **62**, 044004 (2000).
21. S. Capstick, W. Roberts, Phys. Rev. D **47**, 1994 (1993).
22. Fl. Stancu, P. Stassart, Phys. Rev. D **38**, 233 (1988).
23. M. Batinic, I. Slaus, A. Svarc, B.M.K. Nefkens, Phys. Rev. C **51**, 2310 (1995); T.P. Vrana, S.A. Dytman, T.-S.H. Lee, Phys. Rep. **328**, 181 (2000).
24. F. Cano, P. González, B. Desplanques, S. Noguera, Z. Phys. A **359**, 315 (1997).